JARQ 55 (2), 137-146 (2021) https://www.jircas.go.jp

Analysis of Salinity Behavior in Hakata Bay after Heavy Rainfall Using a Three-dimensional σ-Coordinate Model

Akihiro FUKUDA[1], Toshinori TABATA[2]*, Kazuaki HIRAMATSU[2] and Masayoshi HARADA[2]

[1] Department of Agro-Environmental Sciences, Graduate School of Bioresource and Bioenvironmental Sciences, Kyushu University, Fukuoka, Japan
[2] Department of Agro-Environmental Sciences, Faculty of Agriculture, Kyushu University, Fukuoka, Japan

Abstract

Massive freshwater discharges due to heavy rainfall have recently caused negative changes to coastal waters, such as red tides and anoxic water masses. In this research, a salinity analysis was conducted using a three-dimensional σ-coordinate model to evaluate the impact of large freshwater discharges on the horizontal and vertical distribution of salinity. Specifically, Hakata Bay was examined after a heavy rainfall with a six-year return period, beginning 16 September 2002, a common recurrence interval. The data were calculated for 11-27 September 2002. Tank models were applied to calculate river inflow discharges, which were considered river inflow in the hydrodynamic and salinity diffusion model for Hakata Bay. Model validation results showed high reproducibility, and the calculated tidal current and salinity agreed well with observed data. Results also showed that: (1) salinity was less than 15.0 psu at the river mouths about one day after heavy rainfall; (2) low-salinity water (< 28.0 psu) spread across the surface of the inner part of the bay; and (3) salinity differences between the surface and bottom were large (approximately 4 psu) and lasted three days after the heavy rainfall. It was concluded that red tides and anoxic water masses could be induced in the inner part of the bay.

Discipline: Agricultural Engineering
Additional key words: coastal sea, freshwater discharge, hydrodynamic and salinity diffusion model, tank model

Introduction

In recent years, global climate change has caused more frequent, heavy rainfalls. Heavy rainfall can cause considerable damage on land through flooding and sediment disasters. Similarly, studies have recently reported negative changes to the water environment, such as red tides and anoxic water masses in semi-enclosed bays (Katano et al. 2012, Kawamura et al. 2013, Jeong et al. 2017). Hakata Bay also has those environmental problems that is reduced by heavy rainfall. It is a semi-enclosed bay located at the metropolis of Fukuoka, a city at the northern end of the island Kyushu in Japan (Fig. 1). Hakata is designated a special major port (Tai et al. 2012), and Hakata Bay is one of the most important harbors in western Japan. The bay has a rich ecosystem due to its vast tidal flats, such as Wajiro Higata and Imazu Higata in its eastern and western parts, respectively. Moreover, migratory birds from other continents frequent the bay (Babazaki et al. 2009), making protecting its environment important. The bay also has a nearby urban area and has experienced negative changes to its ecosystem and environmental degradation of its coastal water by red tides and local anoxic water masses. Yanagi & Ishii (2009) reported that a large nutrient inflow after a heavy rainfall in June 2004 caused a red tide, which induced an anoxic water mass in inner Hakata Bay by reducing the light intensity in the water column. The bay is important as a harbor and a valuable ecosystem, making its water environment issues vitally important.

A few studies have examined the impacts of a massive freshwater discharges into coastal water due to heavy rainfall. Among them, Murakami et al. (2007) discussed flow and density structures in Ise Bay in the

*Corresponding author: ttabata@bpes.kyushu-u.ac.jp
Received 15 October 2019; accepted 21 July 2020.

Tokai area of Japan after a record rainfall. To do so, they used numerical analysis with a coupled Atmosphere-Ocean-Wave model, which showed that the massive freshwater discharge completely changed the current and density structure of Ise Bay. Kanzaki et al. (2015) investigated the behavior of river water discharged into the Ariake Sea in the northern part of Kyushu after heavy rainfall in July 2012 using a three-dimensional hydrodynamic and diffusion model. This research found strong salinity stratification in Ariake Bay with a 20-30 psu difference between the surface and the bottom. These few examples concentrated on the impact of a massive freshwater discharge into coastal waters. Although many studies have constructed three-dimensional models of Hakata Bay (Yokoyama et al. 2014), no study has examined large freshwater behavior after a heavy rainfall because it is so difficult to make field observations in coastal areas after a heavy rain, so there is not sufficient information for solving the environmental degradation problem of coastal water due to large freshwater discharges. The reasons include the short-term inflow of large nutrient loads and strong salinity stratification due to a large amount of freshwater discharge from rivers (Tsutsumi et al. 2003). Another cause is that floc releases microalgae into sea water because sea water with low salinity decomposes floc (Isagai 2014). Hence, salinity behavior controls the physical and chemical environment in a coastal water body and the three-dimensional distribution of salinity must be understood. It is important to evaluate the impact of heavy rains occurring frequently in semi-enclosed bays, so three-dimensional salinity modeling is essential.

Fukuda et al. (2017) conducted a two-dimensional numerical analysis of salinity behavior in Hakata Bay after a heavy rainfall. Though the study demonstrated a rough trend in the horizontal behavior of large freshwater discharge, it is necessary to also evaluate the vertical structure of salinity. The current study analyzed salinity behavior in Hakata Bay after a heavy rainfall event with a six-year return period, a common recurrence period. A three-dimensional σ-coordinate model that is widely applied to numerical modelling of coastal seas (Takioka et al. 2006, Murakami et al. 2013) was used. Tank models were applied to calculate river inflow discharges in a hydrodynamic and salinity diffusion model of Hakata Bay. Model validation showed high reproducibility. The study evaluated the impact of large freshwater discharges on the horizontal and vertical distribution of salinity.

Materials and methods

1. Target area

Hakata Bay, which is located in the city of Fukuoka on the northern end of Kyushu in Japan (Fig. 1), has a sea

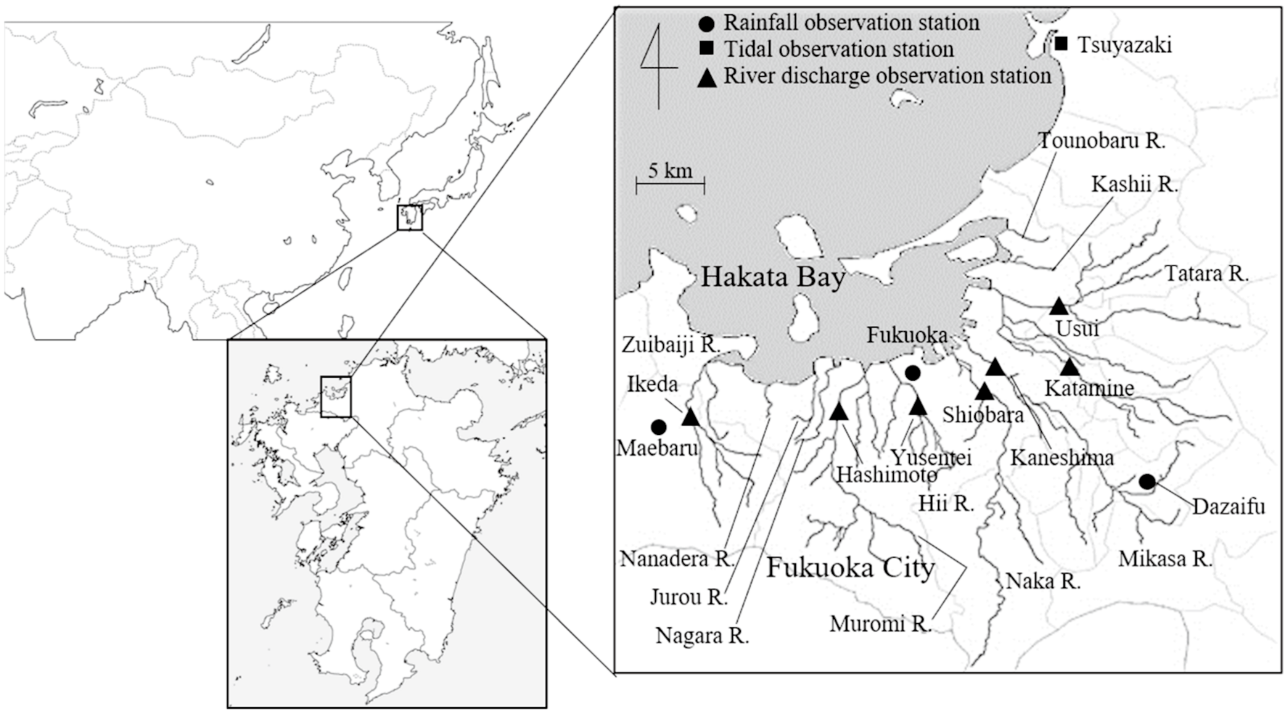

Fig. 1. Map of Hakata Bay

The filled circles, square and triangle indicate the locations of rainfall observation stations, tidal observation station, and river discharge observation point of the Zuibaiji River, respectively. Gray lines indicate rivers flowing into the bay.

surface area of 133.3 km^2, a mean depth of 10.8 m, and a maximum depth of approximately 23 m (Fukuoka City Environmental Bureau 2016). Its geographical enclosed index is 2.04 (International EMECS Center 2001). Because shallow water spreads widely in the bay, tidal flats such as Imazu Higata and Wajiro Higata have formed, resulting in a variety of ecosystems across the bay. The bay is fed by six main rivers: Tatara, Mikasa, Naka, Hii, Muromi, and Zuibaiji, and there have been few observations of river discharge. In the past, excessive nitrogen and phosphorus inflow from domestic wastewater associated with Fukuoka industrial development greatly damaged the bay's water environment, causing widespread red tides and water anoxic masses. Advanced sewage treatment of the city has since reduced nutrient concentration and restrained primary production in the bay (Yokoyama et al. 2011). However, the bay still has water quality issues due to large river inflow discharges after heavy rainfall, which damage the ecosystems and aquatic resources.

Tidal current vectors and salinities were observed by the Fukuoka City Port and Harbor Bureau only 30 July 2007. In addition, the Fukuoka City Environmental Bureau has measured water quality only once a month, with which the impact of heavy rainfall can't be evaluated. To help protect the environment of a shallow coastal area such as Hakata Bay, hydrodynamic and diffusion models are essential. It is necessary to track three-dimensional salinity behavior, especially after heavy rainfalls when a massive amount of freshwater discharge occurs.

2. Model description

Three-dimensional σ-coordinate models (Phillips 1957) are generally used to analyze salinity behavior in coastal seas (Irie et al. 2003, Serio et al. 2007). In this research, a σ-coordinate system was incorporated with a hydrodynamic and salinity diffusion model to accurately represent how the shallow inner part of the bay was influenced by freshwater river inflow discharge.

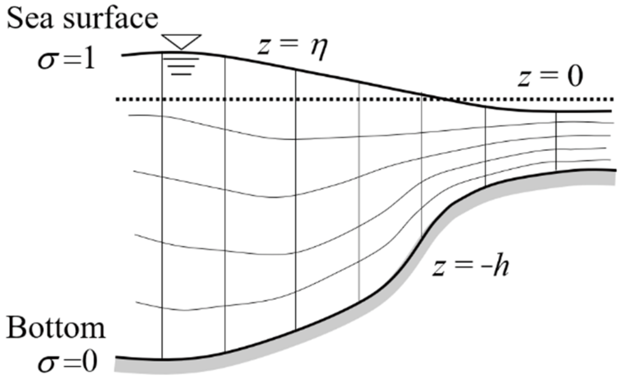

Fig. 2. Conceptual diagram of the σ-coordinate system

In the Cartesian co-ordinate system, the sea surface and bottom are defined as $z=\eta$ and $z=-h$, respectively. In the σ-coordinate system, the sea surface and bottom are σ=1 and σ=0, respectively (Fig. 2), wherein the coordinate conversion formula is

$$\sigma=\frac{z+h}{h+\eta} \tag{1}$$

In the σ-coordinate system, the number of vertical layers is constant regardless of water depth. This coordinate system makes a model more versatile, allowing it to retain the vertical structure of shallow areas while more accurately simulating flow fields near the bottom than the Cartesian co-ordinate system (Sasaki 1998). Therefore, the model can effectively calculate salinity behavior after a heavy rainfall in shallow areas such as river mouths and inner areas of bays.

The model-governing equations were composed of the continuity equation for an incompressible fluid (Eq. 2), the Reynolds equation using a hydrostatic pressure approximation (Eqs. 3 and 4), and the diffusion equation of salinity (Eq. 5) with the σ-coordinate conversion, as follows:

$$\frac{\partial \eta^*}{\partial t}+\int_0^1 \frac{\partial \tilde{u}^*}{\partial x}\,d\sigma+\int_0^1 \frac{\partial \tilde{v}^*}{\partial y}\,d\sigma=0 \tag{2}$$

$$\begin{aligned}&\frac{\partial \tilde{u}^*}{\partial t}+\frac{\partial (Huu)}{\partial x}+\frac{\partial (Huv)}{\partial y}+\frac{\partial (w_s\tilde{u}^*)}{\partial \sigma}\\ &=Hfv-\frac{gH}{\rho}\left[(\rho_0+\rho'\sigma)\frac{\partial \eta^*}{\partial x}\right.\\ &\left.+\rho'(\sigma-1)\frac{\partial h}{\partial x}+\frac{\partial}{\partial x}\left\{(\eta^*+h)\int_\sigma^1 \rho' d\sigma\right\}\right]\\ &+\frac{1}{H^2}\frac{\partial}{\partial \sigma}\left(A\sigma\frac{\partial \tilde{u}^*}{\partial \sigma}\right)+HA_H\left(\frac{\partial^2 u}{\partial x^2}+\frac{\partial^2 u}{\partial y^2}\right)\end{aligned} \tag{3}$$

$$\begin{aligned}&\frac{\partial \tilde{v}^*}{\partial t}+\frac{\partial (Huv)}{\partial x}+\frac{\partial (Hvv)}{\partial y}+\frac{\partial (w_s\tilde{v}^*)}{\partial \sigma}\\ &=-Hfu-\frac{gH}{\rho}\left[(\rho_0+\rho'\sigma)\frac{\partial \eta^*}{\partial y}\right.\\ &\left.+\rho'(\sigma-1)\frac{\partial h}{\partial y}+\frac{\partial}{\partial y}\left\{(\eta^*+h)\int_\sigma^1 \rho' d\sigma\right\}\right]\\ &+\frac{1}{H^2}\frac{\partial}{\partial \sigma}\left(A_\sigma\frac{\partial \tilde{v}^*}{\partial \sigma}\right)+HA_H\left(\frac{\partial^2 v}{\partial x^2}+\frac{\partial^2 v}{\partial y^2}\right)\end{aligned} \tag{4}$$

$$\begin{aligned}&\frac{\partial (HS^*)}{\partial t}+\frac{\partial (HuS)}{\partial x}+\frac{\partial (HvS)}{\partial y}+\frac{\partial (Hw_s S^*)}{\partial \sigma}\\ &=\frac{1}{H^2}\frac{\partial}{\partial \sigma}\left(K_\sigma\frac{\partial (HS^*)}{\partial \sigma}\right)+HK_H\left(\frac{\partial^2 S}{\partial x^2}+\frac{\partial^2 S}{\partial y^2}\right)\end{aligned} \tag{5}$$

where t is time (s); u and v are velocity components in the x- and y-directions (m/s); H ($=\eta + h$) is the depth from the bottom to the sea surface (m); ρ ($= \rho_0 + \rho'$), ρ_0, and ρ' are density, standard ρ, and the difference between ρ and ρ_0, respectively (kg/m^3); g is the gravitational constant (m/s^2); f is the Coriolis parameter (1/s); $\tilde{u}$ and $\tilde{v}$ are line discharges in the x- and y-directions, respectively (m^2/s; $\tilde{u} = uH$ and $\tilde{v} = vH$); A_H and K_H are the horizontal eddy viscosity and diffusivity coefficients, respectively (m^2/s); A_σ and K_σ are the vertical eddy viscosity and diffusivity coefficients, respectively (m^2/s); and S is salinity (psu). w_s is the velocity component in the σ-direction (1/s) and expressed as follows:

$$w_s = \frac{1}{H}\left[\sigma\int_0^1 \frac{\partial (Hu)}{\partial x}\,d\sigma + \sigma\int_0^1 \frac{\partial (Hv)}{\partial y}\,d\sigma - \int_0^\sigma \frac{\partial (Hu)}{\partial x}\,d\sigma - \int_0^\sigma \frac{\partial (Hv)}{\partial y}\,d\sigma\right] \tag{6}$$

For the numerical solution, the semi-implicit method algorithm of Sasaki et al. (1996) was utilized. This method is what implicitly discretizes variables with * such as sea surface elevation η, line discharges, and the vertical convective and viscosity (diffusive) salinity term.

The horizonal eddy viscosity (A_H) and diffusivity (K_H) coefficients were determined using the Smagorinsky model (Smagorinsky 1963):

$$A_H = K_H = \frac{1}{2} S_m A_G \left\{\left(\frac{\partial u}{\partial x}\right)^2 + \frac{1}{2}\left(\frac{\partial v}{\partial x} + \frac{\partial u}{\partial y}\right)^2 + \left(\frac{\partial v}{\partial y}\right)^2\right\}^{\frac{1}{2}} \tag{7}$$

where S_m (=0.2) is the model parameter and A_G (m^2) is mesh size.

The vertical eddy viscosity (A_σ) and diffusivity (K_σ) coefficients were determined using Kolmogorov's hypothesis (Kowalik & Murty 1993):

$$A_\sigma = l^2 \left[\left(\frac{\partial u}{\partial z}\right)^2 + \left(\frac{\partial v}{\partial z}\right)^2\right]^{\frac{1}{2}} \sqrt{1 + \frac{R_i}{P_r}} \tag{8}$$

$$K_\sigma = \frac{A_z}{P_r} \tag{9}$$

where R_i is the Richardson number, P_r is the turbulent Prandtl number, and l (m) is the mixing length. The turbulent number P_r was determined by the following expression (Kondo et al. 1979):

$$\frac{1}{P_r} = \left\{6.73R_i + \frac{1}{1 + 6.873R_i}\right\}^{-1} \qquad R_i \le 1.0$$
$$= (7R_i)^{-1} \qquad R_i > 1.0 \tag{10}$$

The mixing length l was determined by the following expression (Blackadar 1962):

$$l = \frac{\kappa\,(z+H)}{\left(1 + \frac{\kappa\,(z+H)}{l_0}\right)} \tag{11}$$

where κ is the Karman's constant and l_0 (m) is the maximum value of l.

Finally, the wet-and-dry method proposed by Uchiyama (2004) was introduced to represent the appearance and disappearance of tidal flats, allowing robust calculation in very shallow areas.

3. Calculation conditions

Figure 3 shows the bathymetry of the calculation area and the river inflow points in Hakata Bay. The calculations were conducted with a spatial discretization of Δx, Δy = 100 m, and 7 vertical layers. A temporal discretization of Δt was set at 20.0 s for low river inflow discharge and 1.0 s for high river inflow discharge to stabilize the calculation near river mouths. At the bay entrance, the tidal level was calculated using harmonic constants obtained at the Tsuyazaki tidal observation station; tidal level was deemed an open boundary condition in the calculation. In order to investigate the effect of freshwater discharge into the coastal area, the wind stress and water temperature was neglected.

In general, it is difficult to observe river discharges, especially after heavy rainfall. The tank model proposed by Sugawara (1985) was applied to determine river inflow discharges during flooding and has been widely used for rainfall-runoff analyses (Noto et al. 2010). In the tank model (Fig. 4), multiple tanks were vertically aligned and orifices were located below and beside each tank. The parameters on the diagram of the tank model in Figure 4 detail the size and height of the orifices, and river discharges were expressed by adjusting the parameters.

The tank models were applied to the six main rivers: Tatara, Mikasa, Naka, Hii, Muromi, and Zuibaiji, which flow into Hakata Bay (Fig. 1). The tank model parameters for the six rivers were identified from hourly observed discharges using trial-and-error. Rainfall data from the Japan Meteorological Agency stations of Fukuoka, Maebaru, and Dazaifu (Fig. 1) were used for the calculation.

River inflow discharges from five other small rivers without observed discharge data were calculated using a tank model obtained at a nearest-neighbor river among the six main rivers. As an example, Figure 4 shows the structure and parameters of the tank model for the Zuibaiji river. A tank model with three tanks and three outlets at the first tank was adopted for flood runoff analyses. Figure 4 also compares the observed and calculated discharges of the Zuibaiji from 25 August to 23 September 2005. A Nash-Sutcliffe (NS) coefficient of 0.94 and Relative Error (RE) of 0.12 indicated that the tank model reproduced the observed data accurately. Tank model calibration results for the other five main rivers were similar, and all tank models exhibited good reproducibility.

This research analyzed the impact of a massive freshwater discharge from rivers due to heavy rainfall in the Hakata Bay region using the three-dimensional σ-coordinate model. The calculation period was set as 11-27 September 2002 because a heavy rainfall produced 163.5 mm/d on 16 September in Fukuoka, which has an estimated six-year return period for rainfall events. The total, peak, and maximum two-hour accumulation of precipitation during the event were 167.0 mm, 39.5 mm/h, and 65.5 mm, respectively, which indicate an intense rainfall. Figure 5 shows the calculated discharge at the Zuibaiji river during that period. Large discharges from eleven river inflow points (Fig. 3) were incorporated into the calculations using the hydrodynamic and salinity diffusion model.

Because salinity data at river mouths were not available, salinity boundary conditions at the river mouths were determined using the ratio between river mouth water depth and an increased depth due to river inflow discharge:

$$S_2 = \frac{S_1\, h_1}{h_1 + h_2} \qquad (12)$$

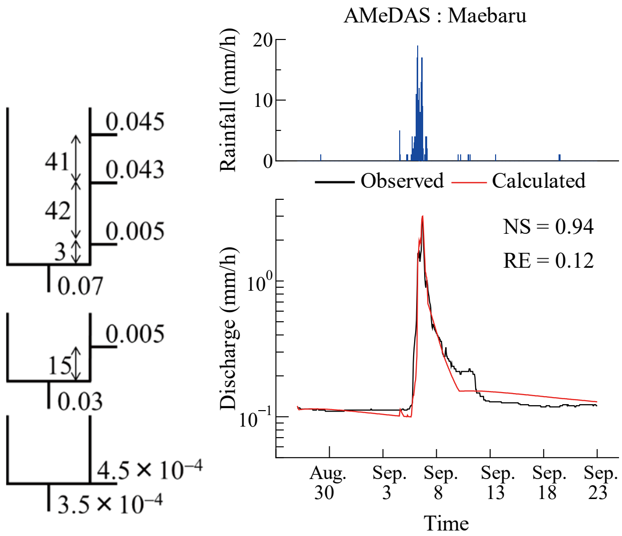

Fig. 4. Tank model used to calculate rainfall-runoff in the Zuibaiji River watershed, and the comparison of observed and calculated discharges at the Ikeda river discharge observation point from 25 August to 23 September 2002

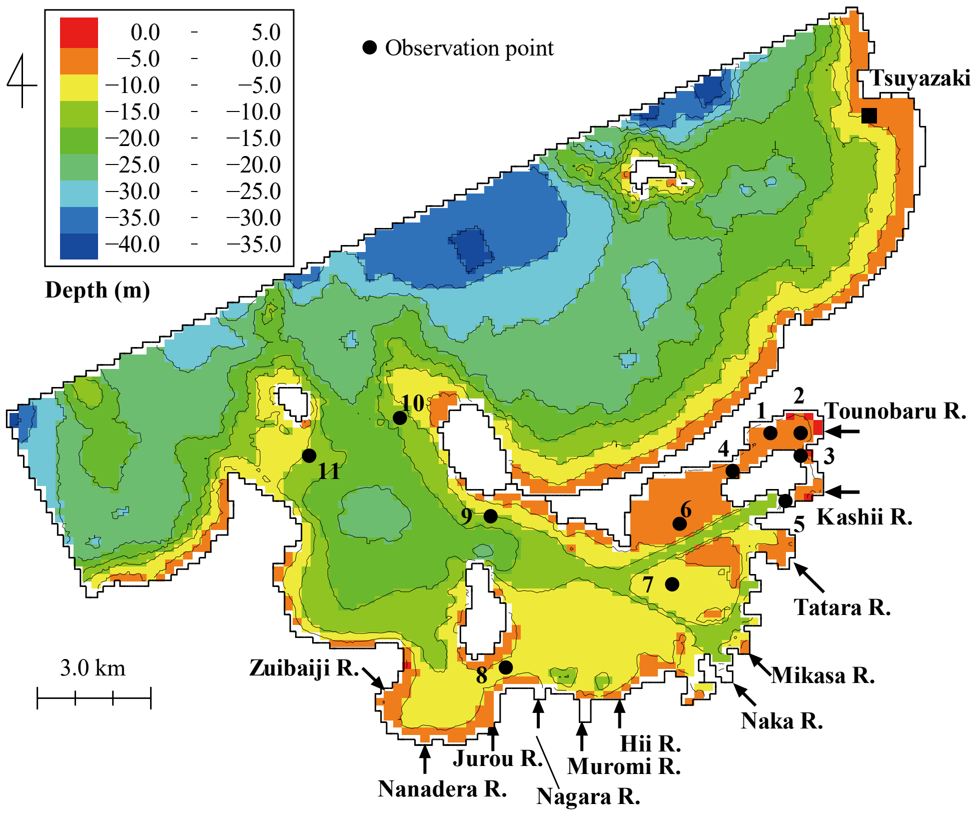

Fig. 3. Bathymetry of the calculation area, as well as the locations of observation points, river inflow points, and the Tsuyazaki tidal observation station

where h_1 is the present water depth, h_2 is the water depth increased by river inflow discharge, S_1 is the initial salinity, and S_2 is the salinity after the inflow discharge.

Prior to simulating the impact of the heavy rainfall event, the hydrodynamic and salinity diffusion model was validated over a two-week period. The validation period was 18 July to 2 August 2007, when the observed tidal current vectors and salinities were available on St. 1 to 11 in Figure 3, and there was almost no rain in Fukuoka.

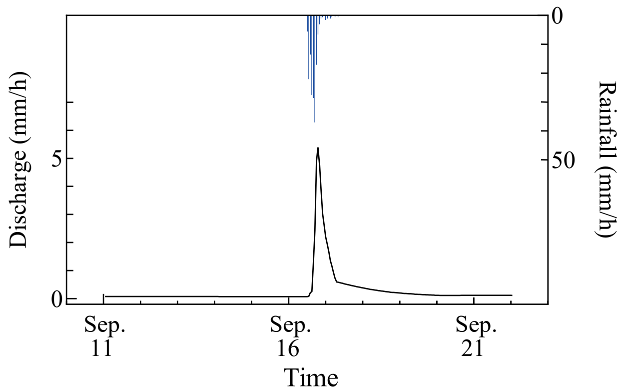

Fig. 5. Calculated discharge at the Ikeda river discharge observation point of the Zuibaiji River from 11-22 September 2002

Results and discussion

1. Model validation

Observation points for velocity and salinity are indicated in Figure 3. Figure 6(a) compares observed and calculated tidal current vectors at one-hour intervals at several observation points from 0:00 to 23:00 on 30 July 2007. The calculated tidal current vectors agreed well with the observed ones. Figure 6(b) compares observed

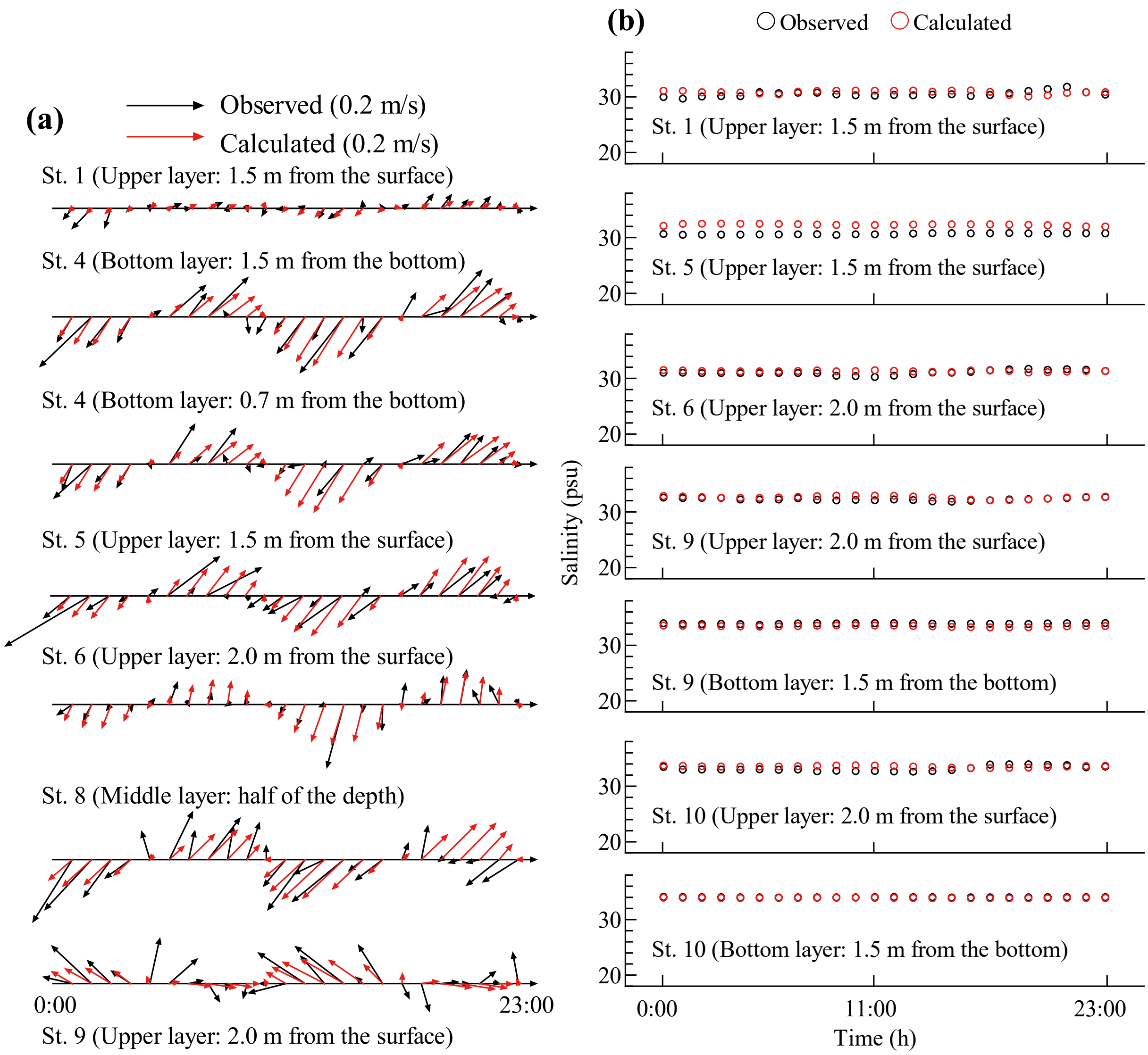

Fig. 6. Comparisons of observed and calculated (a) tidal current vectors and (b) salinities, in one-hour intervals from 0:00 to 23:00 on 30 July 2007

and calculated salinity values at several observation points for the same period as the tidal current vectors. The calculated salinities at St. 5 were slightly higher than observed values. Bathymetry suddenly changed near St.5. It is known that the σ-coordinate model causes errors when the seabed suddenly changes. Also, there are small rivers that could not be considered in the model. However, the other calculated salinities demonstrated good agreement with observed values. Overall, the validation results indicated that the hydrodynamic and salinity diffusion model performed well in simulating tidal currents and salinity diffusion in Hakata Bay.

2. Post-rainfall salinity analysis

Figure 7 shows salinity calculation results. The horizontal distribution of salinity is shown at the (a) surface layer and (b) bottom layer (1) before the heavy rainfall (0:00 16 September 2002), (2) after the heavy rainfall (20:00 17 September 2002), and (3) one week after the heavy rainfall (23:00 24 September 2002). Comparing Figure 7(1-a) and Figure 7(2-a), a very low salinity of less than 15.0 psu was found at the river mouths because substantial amounts of fresh water flowed into the bay over a short period. However, according to Figure 7(2-a) and Figure 7(3-a), fresh water spread out wider, and low-salinity water of less than 28 psu covered the entire inner part of the bay, reaching the outer bay one week after the heavy rainfall (Fig. 7(3-a)). Fresh water flowing into the bay took some time to spread out, and low-salinity water (< 28.0 psu) was concentrated at the large river mouths (Fig. 3). Since tank models were utilized for the six main rivers that flow into Hakata Bay, it can be said that the model reproduced the inflow dynamics of freshwater discharges quite well. In this analysis, the six-year probability rainfall, a relatively frequent rainfall, was targeted and there is almost no rainfall before or after the event. Therefore, it is expected that similar outflow patterns will be obtained when such a sudden heavy rain occurs in Fukuoka. In that case, similar phenomena are expected when Fukuoka experiences heavy rainfall.

At the bottom (Figs. 7(1-b) and 7(2-b)), only slight differences were evident immediately after the heavy rainfall. However, low-salinity water spread evenly over the bottom during the week after the heavy rainfall (Fig. 7(3-b)). We could therefore surmise that low-salinity water spreading at the surface mixed vertically and reached the bottom. Furthermore, salinity differences between the surface and bottom in central and western Hakata Bay were larger than those in the eastern part, so the strength of mixing between the surface and the bottom in the eastern part was greater than that in the central and western part. This may be caused by the difference in the discharges from the rivers. The Tatara and Naka rivers have the biggest discharge of all. Moreover, the east area is shallower than the west area is, as shown in Figure 3. This enormous discharge and depth difference induced the mixing in east area. As a result, salinity stratification occurred more easily in central and western Hakata Bay. Figure 8 shows a salinity time series during the calculation period at St. 7 (Fig. 3). Roughly one day after the heavy rainfall, the salinity difference between the surface and bottom was large, about 4 psu. Surface salinity suddenly decreased during the heavy rainfall then slowly increased with evident tide fluctuations. However, the bottom salinity slowly decreased and the difference became gradually smaller over one week.

Abe et al. (2013) found good linearity between salinity and nutrient concentrations at the surface, using short-term observations after a heavy rainfall at the center of the Seto Sea. Their results indicated that the relationship between salinity and nutrient concentrations at the sea surface could be deciphered immediately after large river discharges. In addition, according to the Fukuoka Fisheries and Marine Technology Research Center (2016), red tides occurred frequently in inner Hakata Bay, especially near the mouths of the Tatara, Mikasa, Naka, Hii, and Murom rivers. Low-salinity water spread across the inner part of Hakata Bay one week after the heavy rainfall (Fig. 7(3-a)). Therefore, it was suspected that nutrients such as nitrogen and phosphorus might spread out similarly, allowing microalgae that absorb nitrogen and phosphorus to also spread throughout the inner bay. Furthermore, salinity stratification occurred approximately three days after the heavy rainfall (Fig. 8). Because salinity stratification reduces vertical mixing, dissolved oxygen at the bottom might be depleted if red tides on the surface prevented sunlight from reaching it. Because the targeted heavy rainfall was estimated over a six-year return period, these environmental effects may also occur with some frequency.

Conclusions

In this research, a three-dimensional σ-coordinate hydrodynamic and salinity diffusion model was applied to analyze the salinity behavior after a heavy rainfall event in Hakata Bay. Sugawara's tank model was used to obtain river inflow discharges at eleven rivers near the bay. Discharge calculated using the tank model exhibited good agreement with observed values. The model's tidal current vectors and salinities also agreed well with observed data over most of the calculation area.

Numerical model results for salinity behavior after the heavy rainfall on 16 September 2002 in Hakata Bay indicated that (1) very low salinity (< 15.0 psu) was found at the river mouths about one day after the heavy rainfall; (2) low-salinity (< 28.0 psu) surface water spread across the inner part of the bay; and (3) the salinity difference between the surface and bottom was large (approximately 4 psu) about one day after the heavy rainfall. The salinity results suggest that nutrient behaviors in the rivers were

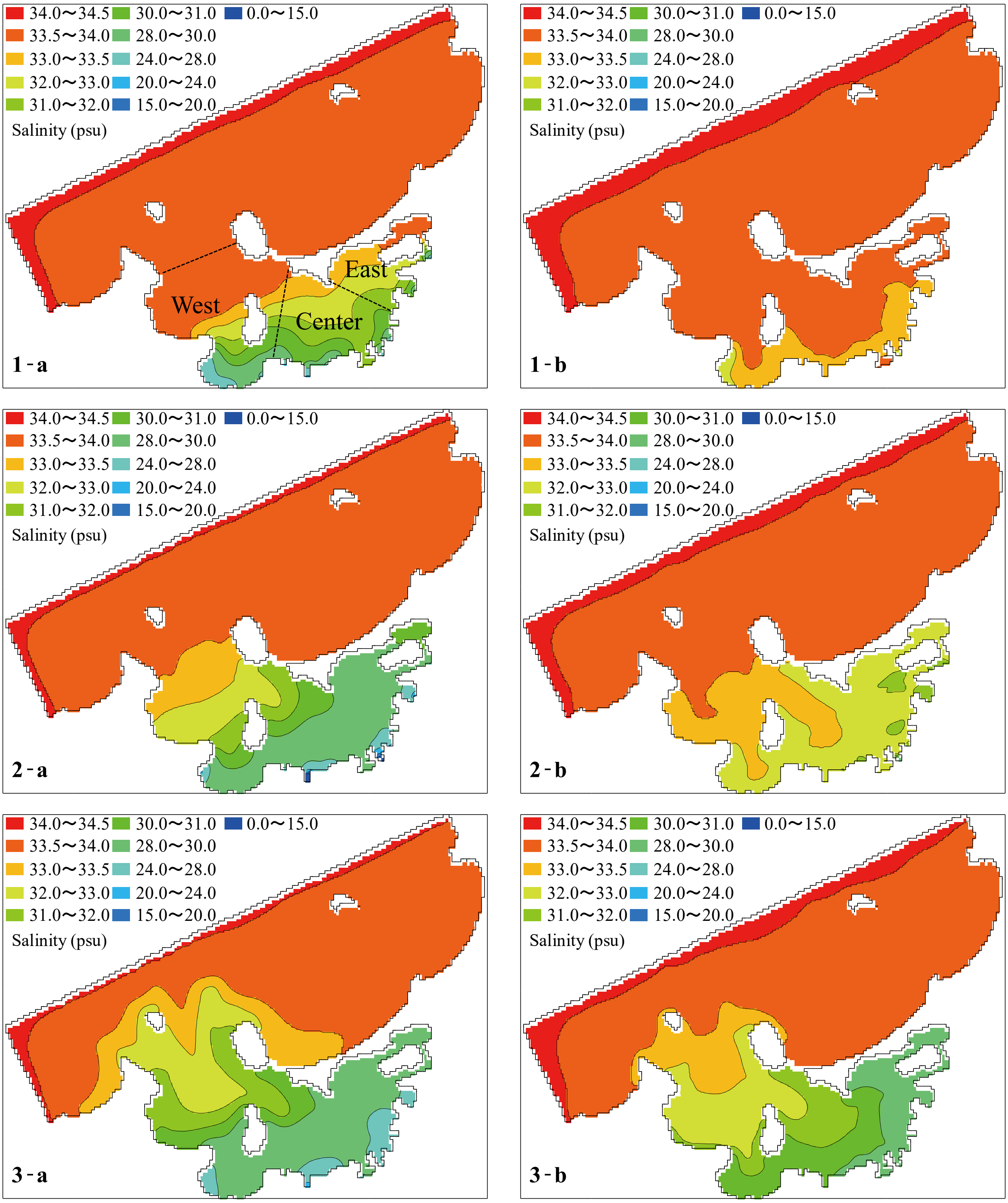

Fig. 7. Salinity distribution at the (a) surface and (b) bottom, at (1) 0:00 16 September (neap flood tide), (2) 20:00 17 September (spring ebb tide), and (3) 23:00 24 September 2002 (spring ebb tide), respectively (See also Fig. 3)

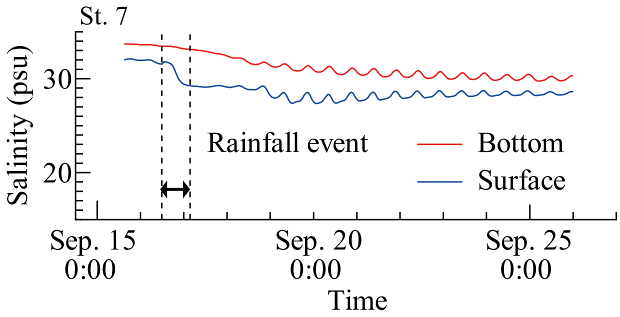

Fig. 8. Time series of calculated salinity at St.7 from 15:00 15 September to 0:00 26 September 2002 (See also Fig. 3)

likely similar, and salinity stratification lasting approximately three days probably reduced vertical mixing in the inner bay area. Consequently, red tides and an anoxic water mass could occur in the inner bay. Because the targeted and frequent heavy rainfalls were estimated over a six-year return period, these environmental changes may also occur frequently. Due to global climate change, the frequency and intensity of rainfall are increasing significantly. These result show that not only land but also coastal areas could be damaged by heavy rainfall and countermeasure must be developed. These findings about large freshwater dynamics in the studied coastal should provide give important knowledge useful in protecting coastal environments.

Acknowledgements

This work was supported by a JSPS Grant-in-Aid for Young Scientists (B) (Grant Number 17K15347), JSPS Grant-in-Aid for Scientific Research (A) (Grant Number 18H03968), and JSPS Grant-in-Aid for JSPS Fellows (Grant Number 19J12512).

References

Abe, K. et al. (2013) High nutrients in the coastal area after heavy rain observed in the central Seto Inland Sea in July 2012. *J. Oceanogr.*, **69**, 269-275.

Babazaki, M. et al. (2009) A case study of mitigation in Mishima Area of Hakata Bay, Fukuoka. *Kankyo Assessment Gakkai-shi (Journal of Japan Society for Impact Assessment)*, **7**, 84-91 [In Japanese].

Blackadar, A. K. (1962) The vertical distribution of wind and turbulent exchange in a neutral atmosphere. *J. Geophys. Res.*, **67**, 3095-3102.

Fukuda, A. et al. (2017) Impact of large fresh water discharges into Hakata Bay due to torrential rain using nested two-dimensional convective-dispersive model. *J. Water Resour. Protect.*, **9**, 553-565.

Fukuoka City Environmental Bureau (2016) *The Second plan of environmental protection of the Hakata Bay.* Fukuoka City, pp. 1-2 [In Japanese].

Fukuoka Fisheries and Marine Technology Research Center (2016) Measurement project of fishery environment protection (2) red tides investigation, *Heisei 28 Nendo Fukuoka-ken Suisan Kaiyou Gijutsu Center Jigyo Houkoku (Project Report of Fukuoka Fisheries And Marine Technology Research Center in FY 2016)*, pp. 77-83 [In Japanese].

International EMECS Center (2001) *Environment guidebook of enclosed bays in Japan (88 bays).* Kobe City [In Japanese].

Irie, M. et al. (2003) Application of improved σ-coordinate model in flow field of large density difference. *Kaigan Kougaku Ronbun-Shu (Proc. Coast. Eng. JSCE)*, **50**, 361-365 [In Japanese].

Isagai, H. (2014) Relationship between salt concentration of Ariake Sea and red tide occurrence after heavy rain. *Shizen Saigai Kenkyu Kyougikai Seibu Chiku Bu-Kaihou: Kenkyu Ronbun-Shu (Western Regional Division report of Natural Disaster Research Council)*, **38**, 13-16 [In Japanese].

Jeong, H. J. et al. (2017) Ichthyotoxic Cochlodinium polykrikoides red tides offshore in the South Sea, Korea in 2014: I. Temporal variations in three-dimensional distributions of red-tide organisms and environmental factors. *Algae*, **32**, 101-130.

Kanzaki, M. et al. (2015) Behavior of river water discharged into Ariake Sea by heavy rainfall in northern part of Kyushu in July 2012. *Doboku Gakkai Ronbun-Shu. B2, Kaigan Kougaku (J.JSCE, Ser.B2, Coastal engineering)*, **71**, 439-444 [In Japanese with English summary].

Katano, T. et al. (2012) Wax and wane of Chattonella (Raphidophyceae) bloom with special reference to competition between Skeletonema (Bacillariophyceae) in the Ariake Sea, Japan. *J. Oceanogr.*, **68**, 497-507.

Kawamura, Y. et al. (2013) Changes of sea condition and influence to fisheries in Saga Ariake Bay after Kyushu Hokubu Heavy Rain in July, 2012. *Saga-ken Ariake Suisan Shinkou Center Kenkyu Houkoku (Bull. Saga Prefect. Ariake Fish. Res. Dev. Cent.)*, **26**, 101-135 [In Japanese].

Kondo, J. et al. (1979): On wind-driven current and temperature profiles with diurnal period in the oceanic planetary boundary layer, *J. Phys. Oceanogr.*, **9**, 360-372.

Kowalik, Z. & Murty, T. S. (1993) *Numerical modeling of ocean dynamics.* World Scientific, P O Box 128, Farrer Road, Singapore 9128.

Murakami, T. et al. (2007) Numerical analysis of flow and density structures in Ise Bay Area at Tokai Heavy Rain. *Kaigan Kougaku Ronbun-Shu (Proc. Coast. Eng. JSCE)*, **54**, 371-375 [In Japanese with English summary].

Murakami, T. et al. (2013) Numerical analysis of sediment transport in Amitori Bay, Iriomote Island, Japan. *Doboku Gakkai Ronbun-Shu. B3, Kaiyou Kaihatsu (J.JSCE, Ser. B3, Ocean engineering)*, **69**, 928-933 [In Japanese with English summary].

Noto, F. et al. (2010) An evaluation of snow storage depth in the Tedori River Basin using tank model., *Nougyou Nouson Kougakkai Ronbun-shu (Trans. of JSIDRE)*, **268**, 31-37 [In Japanese with English summary].

Phillips, N. A. (1957) A coordinate system having some special advantages for numerical forecasting. *Journal of Meteorology*, **14**, 184-185.

Sasaki, J. et al. (1996) Study on scale of blue tide in Tokyo Bay. *Kaigan Kougaku Ronbun-Shu (Proc. Coast. Eng. JSCE)*, **43**, 1111-1115 [In Japanese].

Sasaki, J. (1998) Numerical modelling of 3-dimensional baroclinic flows in bays. *In* Suikougaku ni kansuru kaki kenshu-kai kougi-shu (Journal of summer workshop about hydraulic engineering) No. **34**, Doboku Gakkai Suikougaku Iinkai (Committee on Hydroscience and Hydraulic Engineering), Nagoya University, B.3.1-B.3.20 [In Japanese].

Serio, F. D. et al. (2007) Circulation in a Southern Italy coastal basin: Modelling and field measurements. *Cont. Shelf Res.*, **27**, 779-797.

Smagorinsky, J. (1963) General circulation experiments with the primitive equations. *Mon. Weather Rev.*, **91**, 99-164.

Sugawara, M. (1985) Tank model—For the derivation of river discharge from rainfall. *Chigaku Zasshi (J. Geogr.)*, **94**, 209-221 [In Japanese with English Summary].

Tai, A. et al. (2012) Effects on tide, tidal current and sediment transport by coastline change in Hakata Bay. *Doboku Gakkai Ronbun-Shu. B3, Kaiyou Kaihatsu (J.JSCE, Ser. B3, Ocean engineering)*, **68**, 744-749 [In Japanese with English summary].

Takioka, K. et al. (2006) Analysis of sea water dynamics and transport of floating larva around the Ryukyu Islands for investigation of the network of broad coastal ecosystem. *Kaigan Kougaku Ronbun-Shu (Proc. Coast. Eng. JSCE)*, **53**, 1151-1155 [In Japanese].

Tsutsumi, H. et al. (2003) Studies of the cross section of water in the innermost areas of Ariake Bay with the recent occurrence of hypoxic water and red tide. *Umi no Kenkyu (Oceanography in Japan)*, **12**, 291-305 [In Japanese with English summary].

Uchiyama, Y. (2004) Wetting and drying scheme based on a modified logarithmic law for three-dimensional terrain-following coastal ocean models. *Kaigan Kougaku Ronbun-Shu (Proc. Coast. Eng. JSCE)*, **51**, 351-355 [In Japanese with English Summary].

Yanagi, T. & Ishii, D. (2009) Generation and disappearance mechanisms of hypoxia in the head of Hakata Bay. *Umi no Kenkyu (Oceanography in Japan)*, **18**, 169-176 [In Japanese with English summary].

Yokoyama, Y. et al. (2011) A change of the species composition of phytoplankton with the variation of nutrient concentration in Hakata Bay. *Doboku Gakkai Ronbun-Shu. B3, Kaiyou Kaihatsu (J.JSCE, Ser.B3, Ocean engineering)*, **67**, 340-345 [In Japanese with English summary].

Yokoyama, Y. et al. (2014) A numerical analysis of the behavior of planktonic larvae of Manila calm in Hakata Bay. *Doboku Gakkai Ronbun-Shu. B3, Kaiyou Kaihatsu (J.JSCE, Ser. B3, Ocean engineering)*, **70**, 1080-1085 [In Japanese with English summary].